Draft version July 4, 2011
Preprint typeset using LaTeX style emulateapj v. 8/13/10

CATASTROPHIC QUENCHING IN $\alpha\Omega$ DYNAMOS REVISITED

Alexander Hubbard[1,2] & Axel Brandenburg[1,3]
[1] NORDITA, AlbaNova University Center, Roslagstullsbacken 23, SE 10691 Stockholm, Sweden
[2] Max Planck Institut für Astronomie, Königstuhl 17, D-69117 Heidelberg, Germany
[3]Department of Astronomy, AlbaNova University Center, Stockholm University, SE 10691 Stockholm, Sweden
Draft version July 4, 2011

ABSTRACT

At large magnetic Reynolds numbers, magnetic helicity evolution plays an important role in astrophysical large-scale dynamos. The recognition of this fact led to the development of the dynamical α quenching formalism, which predicts catastrophically low mean fields in open systems. Here we show that in oscillatory $\alpha\Omega$ dynamos this formalism predicts an unphysical magnetic helicity transfer between scales. An alternative technique is proposed where this artifact is removed by using the evolution equation for the magnetic helicity of the total field in the shearing–advective gauge. In the traditional dynamical α quenching formalism, this can be described as an additional magnetic helicity flux of small-scale fields that does not appear in homogeneous α^2 dynamos. In $\alpha\Omega$ dynamos, the alternative formalism is shown to lead to larger saturation fields than previously obtained with the traditional formalism.
Subject headings: MHD — turbulence — Sun: magnetic fields

1. INTRODUCTION

While the possibility, and indeed need, for astrophysical dynamos was recognized quite early (Larmor 1919), the study of dynamos has since been troubled by a number of problems. Cowling's anti-dynamo theorem (Cowling 1933) initially appeared to demonstrate that the entire concept was impossible, though Parker (1955) eventually discovered the physics behind what has come to be called the α effect. Cowling's anti-dynamo theorem was finally shown to be largely inapplicable by analytically solvable dynamos such as the Herzenberg dynamo (Herzenberg 1958). Once the possibility of dynamo action was demonstrated, the development of mean-field α dynamo theory followed (Steenbeck et al. 1966), which describes the generation of poloidal field from toroidal fields.

While the generation of toroidal magnetic fields from sheared poloidal fields is straightforward through the Ω effect, the reverse process is tricky. Without it however, dynamo action is impossible. The α effect, which relies on helicity (twist) in the fluid motion, allows for the generation of strong large-scale magnetic fields such as those observed in the Universe. It can drive dynamo action on its own (α^2 systems), but as shear is ubiquitous in astrophysics, shear-amplified dynamo action is generally expected to outperform α^2 dynamos. Accordingly, $\alpha\Omega$ dynamos, which combine the effects, are expected to be the dominant type of natural astrophysical dynamo (Hubbard & Brandenburg 2011).

More recently however, there were indications, first suggested by Vainshtein & Cattaneo (1992), that the α effect decreases catastrophically already for weak mean fields in the limit of large magnetic Reynolds number (i.e. low non-dimensionalized resistivities). Such behavior would imply that mean-field dynamos driven by the α effect could not generate the observed large-scale magnetic fields. This claim stymied the field of large-scale dynamos for the 1990s. While strong fields are observed in nature, the theoretical understanding appeared to have been cut down. Eventually it was recognized that this behavior is not generally applicable, being restricted to two-dimensional systems, or to homogeneous (non-dynamo generated) mean fields (Blackman & Brandenburg 2002), and large-scale dynamo simulations became common (Brandenburg 2001; Brandenburg & Dobler 2001). These new simulations occurred alongside the realization that magnetic helicity conservation, through the dynamical α quenching formalism, provides an excellent theoretical understanding of the saturation of α–effect dynamos: the build-up of small-scale magnetic helicity quenches the α effect (Field & Blackman 2002). Even so, the question of catastrophic quenching has remained open, with indications of saturated large-scale field strength decreasing with increasing magnetic Reynolds number for shearing sheets and open α^2 systems (Brandenburg & Subramanian 2005; Guerrero et al. 2010). Further, while the saturation field strength in α^2 systems with periodic or perfectly conducting boundaries has been found to be independent of the resistivity for adequately (and in practice modestly) super-critical Re_M, the time scale to reach saturation increases linearly with Re_M (Brandenburg 2001). This has led to the study of magnetic helicity fluxes (Vishniac & Cho 2001; Brandenburg & Sandin 2004; Mitra et al. 2010; Candelaresi et al. 2011), where the hope is that, because the build-up of small-scale magnetic helicity quenches the α effect, stronger and faster growing dynamos should be possible if the helicity is, instead, exported (as it cannot be non-resistively destroyed).

Probing the reality of catastrophic quenching is naturally difficult. Analytical theory is impossible, and direct numerical simulations are limited to Re_M that, while significantly super-critical for many systems, are nevertheless orders of magnitude below those of astrophysical

alex.i.hubbard@gmail.com

systems. The dynamical α quenching formalism allows probing large Re_M in systems it can handle, but its validity there cannot, of course, be directly verified. While the evidence for and against catastrophic quenching is limited, resolving the issue is a crucial step in advancing dynamo theory.

The continued improvement in techniques to measure turbulent dynamo coefficients from simulations have enabled new approaches to evaluating different formulations of the dynamical quenching formalism. In particular, the test-field method (Schrinner et al. 2005, 2007) has been used to rule out the possibility of catastrophic quenching of the turbulent magnetic diffusivity η_t in α^2 dynamos (Brandenburg et al. 2008a). Recent advances in the theory of magnetic helicity fluxes in the presence of shear (Hubbard & Brandenburg 2011) have led us to continue these developments in dynamical quenching by revisiting earlier results from shearing systems. Somewhat surprisingly, these developments return the 1-D α dependent models to the first 0-D α dependent models (Blackman & Brandenburg 2002). In addition, we shall extend here earlier numerical studies of α^2 dynamos in open systems.

2. MEAN-FIELD MODELING

2.1. *Mean-field dynamo action*

We reproduce here some basic results of mean-field modeling. The dynamos we will consider are in the family of α^2, $\alpha\Omega$, and $\alpha^2\Omega$ dynamos, i.e. dynamos where the conversion of toroidal field to poloidal field occurs through the α effect, while the conversion of poloidal to toroidal field occurs through the α effect, the Ω effect, and a combination of the two. In practice, because some conversion of poloidal field to toroidal field through the α effect is always present, $\alpha\Omega$ dynamos are an approximation in the limit that the Ω effect is much stronger than the α effect. All three dynamos, in an infinite, (shearing-) periodic system arise from the same eigenvalue problem.

Although we will focus in this work on the discussion of results from numerical simulations, these results are better understood in terms of linear theory. We assume a standard, isotropic homogeneous α, turbulent resistivity η_t, and consider a system with shear velocity $\boldsymbol{U}_S = Sx\hat{\boldsymbol{y}}$. Under those conditions, the mean-field problem for a one-dimensional $\alpha^2\Omega$ dynamo with $k_x = k_y = 0$ and $k_z = k$ (i.e., averaging over the xy-plane) reduces to the eigenvalue problem

$$\lambda\hat{\boldsymbol{B}} = \begin{pmatrix} -\eta_{\rm T}k^2 & -\mathrm{i}\alpha k & 0 \\ \mathrm{i}\alpha k + S & -\eta_{\rm T}k^2 & 0 \\ 0 & 0 & -\eta_{\rm T}k^2 \end{pmatrix} \hat{\boldsymbol{B}}. \tag{1}$$

where $\eta_{\rm T} = \eta + \eta_t$ is the total, resistive and turbulent, resistivity. The growing mode has eigenvalue and eigenvector

$$\lambda = |\alpha k|\sqrt{1 - \mathrm{i}Q} - \eta_{\rm T}k^2, \tag{2}$$

$$\overline{\boldsymbol{B}} = B_0 \left(\sin kz, \mathrm{sgn}\,(\alpha k)(1+Q^2)^{1/4}\sin(kz+\phi), 0\right), \tag{3}$$

where

$$Q \equiv \frac{S}{\alpha k} \tag{4}$$

is a measure of the relative shear and

$$\phi = 1/2 \arctan Q \tag{5}$$

is the phase between $\overline{B}_x$ and $\overline{B}_y$. The growth rate of the $\alpha^2\Omega$ mode is $\Re\lambda = |\alpha k|\sqrt{(1+(1+Q^2)^{1/2})/2} - \eta_{\rm T}k^2$.

From the above, we draw some significant conclusions true for both $\alpha\Omega$ and the more general $\alpha^2\Omega$ fields:

$$|\overline{h}_m| = |\overline{\boldsymbol{A}}\cdot\overline{\boldsymbol{B}}| = \left|\frac{(1+Q^2)^{1/4}}{k}B_0^2\sin\phi\right|, \tag{6}$$

$$\overline{\boldsymbol{B}}^2 = B_0^2\left(\sin^2 kz + (1+Q^2)^{1/2}\sin^2[kz+\phi]\right), \tag{7}$$

i.e., the magnetic helicity density and the current helicity density $C_m \equiv \overline{\boldsymbol{J}}\cdot\overline{\boldsymbol{B}}$ of the mean-field are spatially uniform, while the amplitude of the mean-field is not spatially uniform if $S \neq 0$ ($Q \neq 0$ and $\phi \neq \pi/2$).

We next make the $\alpha\Omega$ approximation, assuming that $|Q| \gg 1$. We also consider only the case of $\alpha, k, S \geq 0$ to simplify notation (the other cases are analogous). This implies that

$$(1+Q^2)^{1/4} \simeq Q^{1/2} \gg 1, \quad \phi = \frac{\pi}{4}, \quad \Re\lambda = |\alpha k|\sqrt{Q/2} - \eta_{\rm T}k^2. \tag{8}$$

At constant $\eta_{\rm T}$ and S then, the system will be stationary for $\alpha = \alpha_c$ such that

$$\alpha_c = \frac{2\eta_{\rm T}^2 k^3}{S}, \quad Q^{1/2} = \sqrt{\frac{1}{2}}\frac{S}{\eta_{\rm T}k^2}. \tag{9}$$

Further, in such a state we have

$$\frac{\overline{h}_m}{\langle\overline{\boldsymbol{B}}^2\rangle} = \frac{2\eta_{\rm T}k}{S}. \tag{10}$$

The α effect from maximally helical turbulence has $\alpha \sim \eta_t k_f$, where k_f is the energy-carrying scale of the turbulence, and so the mean magnetic field of an $\alpha\Omega$ dynamo is expected to have very low helicity. As we will see, this is an important consideration.

2.2. *Catastrophic α–quenching*

Given the level of interest, it should be noted that "catastrophic" α–quenching has not been consistently defined. We will choose the following definitions:

- Type 1 catastrophic quenching is probably the most extreme case. Here, the *saturated mean-field strength* varies inversely with Re_M (or some non-negligible negative power or similar).
- Type 2 catastrophic quenching is well understood in an α^2 dynamo in a triply-periodic setup as discussed in Section 2.3. Here, the *time* required for final saturation scales linearly with Re_M (or some non-negligible positive power thereof).

A well known example of Type 2 catastrophic quenching is seen in the simulations of Brandenburg (2001), while Type 1 catastrophic quenching has been suspected to occur in the simulations of Brandenburg & Dobler (2001); Brandenburg & Subramanian (2005), but this will be challenged by the present work.

It should be noted that both Type 1 and 2 quenchings might be less than fully catastrophic in practice. A

system which rapidly reaches an Re_M-independent field strength and then resistively decays could be Type 1 and yet have a significant field for all relevant times. Similarly, a system could take a prohibitive resistive time to fully saturate, but already reach significant field strengths on dynamical times.

Given the name α–quenching, it would be appropriate to define a quenching type based on the value of α. Such a definition is quite difficult however, as in the saturated regime the dynamo-driving effect counterbalances resistive decay, so the *net* dynamo-driving terms, including the turbulent resistivity that must accompany an α-effect, are expected to vary with η (and so with Re_M^{-1}).

2.3. *Dynamical α–quenching*

Dynamical α–quenching is a theoretical advance that uses the magnetic α-effect of Pouquet et al. (1976). Under that hypothesis, the actual α effect in a system can be decomposed into a component due to the kinetic effect, α_K, and a component due to the backreaction of the magnetic fields on the flow, α_M:

$$\alpha = \alpha_K + \alpha_M, \quad \alpha_K \simeq -\frac{\tau}{3}\langle \boldsymbol{\omega}\cdot\boldsymbol{u}\rangle, \qquad \alpha_M = \frac{\tau}{3\rho}\langle \boldsymbol{j}\cdot\boldsymbol{b}\rangle. \tag{11}$$

The mean current helicity density of the small-scale field, $\langle \boldsymbol{j}\cdot\boldsymbol{b}\rangle$, is not a tractable quantity but in general it is well approximated by the mean magnetic helicity density of the small-scale field, $\langle \boldsymbol{a}\cdot\boldsymbol{b}\rangle$, through $\langle \boldsymbol{j}\cdot\boldsymbol{b}\rangle \simeq k_f^2\langle \boldsymbol{a}\cdot\boldsymbol{b}\rangle$; see Mitra et al. (2010) for results in an inhomogeneous system. Note that under this definition, *small-scale magnetic helicity* is a *mean* quantity.

The mean small-scale magnetic helicity can be found by subtracting the evolution equation of the large-scale magnetic helicity from that of the total helicity. This takes the form

$$\frac{\partial \overline{h}}{\partial t} = -2\eta\overline{\boldsymbol{J}\cdot\boldsymbol{B}} - \boldsymbol{\nabla}\cdot\overline{\boldsymbol{\mathcal{F}}}, \tag{12}$$

$$\frac{\partial \overline{h}_m}{\partial t} = 2\overline{\boldsymbol{\mathcal{E}}}\cdot\overline{\boldsymbol{B}} - 2\eta\overline{\boldsymbol{J}}\cdot\overline{\boldsymbol{B}} - \boldsymbol{\nabla}\cdot\overline{\boldsymbol{\mathcal{F}}}_m, \tag{13}$$

$$\frac{\partial \overline{h}_f}{\partial t} = -2\overline{\boldsymbol{\mathcal{E}}}\cdot\overline{\boldsymbol{B}} - 2\eta\overline{\boldsymbol{j}\cdot\boldsymbol{b}} - \boldsymbol{\nabla}\cdot\overline{\boldsymbol{\mathcal{F}}}_f, \tag{14}$$

where $\overline{\boldsymbol{\mathcal{F}}} = \overline{\boldsymbol{\mathcal{F}}}_m + \overline{\boldsymbol{\mathcal{F}}}_f$ is the sum of large-scale and small-scale magnetic helicity fluxes and $\overline{\boldsymbol{\mathcal{E}}} \equiv \overline{\boldsymbol{u}\times\boldsymbol{b}}$. Equation (1) assumes that $\overline{\boldsymbol{\mathcal{E}}} = \alpha\overline{\boldsymbol{B}} - \eta_t\overline{\boldsymbol{J}}$. Under the hypothesis that $\langle \boldsymbol{j}\cdot\boldsymbol{b}\rangle \simeq k_f^2\langle \boldsymbol{a}\cdot\boldsymbol{b}\rangle$, Equation (14) can be evolved in a mean-field simulation if a form for the flux term is assumed. We call this *traditional* dynamical α–quenching. In homogeneous, periodic systems, such as homogeneous α^2 dynamos in triply periodic cubes, the flux term vanishes, and the concept behind dynamical α–quenching can be tested. The application of dynamical α–quenching to this system predicts Type 2 quenching: there is an exponential growth phase which ends when $\overline{B}^2/B_{\mathrm{eq}}^2 = k_1/k_f$ (Blackman & Brandenburg 2002). Subsequently, there is a resistively controlled saturation phase with time $1/2\eta k_1^2$, finally ending at a saturated field strength of $\overline{B}^2/B_{\mathrm{eq}}^2 = k_f/k_1$.

Recent work suggests that the appropriate *ansatz* for the flux of mean small-scale magnetic helicity is diffusive, with sub-turbulent diffusion coefficients (Hubbard & Brandenburg 2010). However, recent work has also demonstrated that shear poses a unique problem which can be seen in the case of a shearing-periodic setup at a moment when all quantities are periodic except for the imposed shear flow $\boldsymbol{U}_S = Sx\,\hat{\boldsymbol{y}}$. In that case, the helicity flux has a horizontal component, $(\boldsymbol{U}_S\times\boldsymbol{B})\times\boldsymbol{A}$, which is not periodic and has a finite divergence. While the existence of this net flux through the shearing-periodic boundaries might be unexpected, the need for it can be simply explained. The solution of an $\alpha^2\Omega$ dynamo has spatially uniform large-scale helicity (Equation (6)), but the $\overline{\boldsymbol{\mathcal{E}}}\cdot\overline{\boldsymbol{B}}$ term in Equation (13) depends on z. A flux term with a finite divergence is required to balance the equation, and is found in linear theory, where Equations (13) and (14) take the form

$$\frac{\partial \overline{h}_m}{\partial t} = 2\overline{\boldsymbol{\mathcal{E}}}\cdot\overline{\boldsymbol{B}} - 2\eta\overline{\boldsymbol{J}}\cdot\overline{\boldsymbol{B}} - \boldsymbol{\nabla}\cdot(\overline{\boldsymbol{\mathcal{F}}}_m - \overline{\boldsymbol{\mathcal{E}}}\times\overline{\boldsymbol{A}}), \tag{15}$$

$$\frac{\partial \overline{h}_f}{\partial t} = -2\overline{\boldsymbol{\mathcal{E}}}\cdot\overline{\boldsymbol{B}} - 2\eta\overline{\boldsymbol{j}\cdot\boldsymbol{b}} - \boldsymbol{\nabla}\cdot(\overline{\boldsymbol{\mathcal{F}}}_f + \overline{\boldsymbol{\mathcal{E}}}\times\overline{\boldsymbol{A}}). \tag{16}$$

When $\overline{\boldsymbol{B}}$ takes the form in (3) and $\overline{\boldsymbol{\mathcal{E}}} = \alpha\overline{\boldsymbol{B}} - \eta_t\overline{\boldsymbol{J}}$, the $\boldsymbol{\nabla}\cdot(\overline{\boldsymbol{\mathcal{E}}}\times\overline{\boldsymbol{A}})$ terms cancel the $\overline{\boldsymbol{\mathcal{E}}}\cdot\overline{\boldsymbol{B}}$ terms.

If the flux term is not correctly handled, we can expect the generation of artificial helicity "hot-spots" through the $\overline{\boldsymbol{\mathcal{E}}}\cdot\overline{\boldsymbol{B}}$ terms, which will non-linearly back-react on the dynamo through Equation (11). While an adequate diffusive flux may be able to smooth out such, this poses a clear potential difficulty in applying dynamical α–quenching to shearing systems.

If a mean-field model is solved in terms of the mean magnetic vector potential $\overline{\boldsymbol{A}}$ however, then $\overline{h}_m$ is known at every time step. Thus, rather than evolving Equation (14), one can evolve Equation (12) to find $\overline{h}_f = \overline{h} - \overline{h}_m$, avoiding the $\overline{\boldsymbol{\mathcal{E}}}\cdot\overline{\boldsymbol{B}}$ terms. One known difficulty with this alternate technique is that spatially homogeneous components of $\boldsymbol{A}$ may develop and cause spurious spatial variation in α_M when the latter is defined in terms of $\overline{\boldsymbol{A}}\cdot\overline{\boldsymbol{B}}$. This can be remedied by subtracting out the volume averaged $\langle\boldsymbol{A}\rangle_V$. We refer to this technique of calculating $\overline{h}_f$ as *alternate* dynamical α–quenching. For systems with no native spatial variations in α, nor any instabilities in the spatial variation of α, this procedure will in practice return one to the first attempts to apply dynamical α–quenching using volume averages (Blackman & Brandenburg 2002).

We use an α^2 dynamo to test alternate dynamical α–quenching against traditional dynamical α–quenching (which, in this system, should be identical as there are no spatial variations and so no fluxes). We show the agreement in Figure 1. The small difference that develops is due to a smaller rms spatial noise of α_M in the alternate quenching case.

2.4. *Investigation procedure*

Catastrophic α–quenching lives in the high Re_M regime, beyond the reach of current direct numerical simulation or laboratory experiment. This makes confirming or disproving its existence impossible. The evidence for

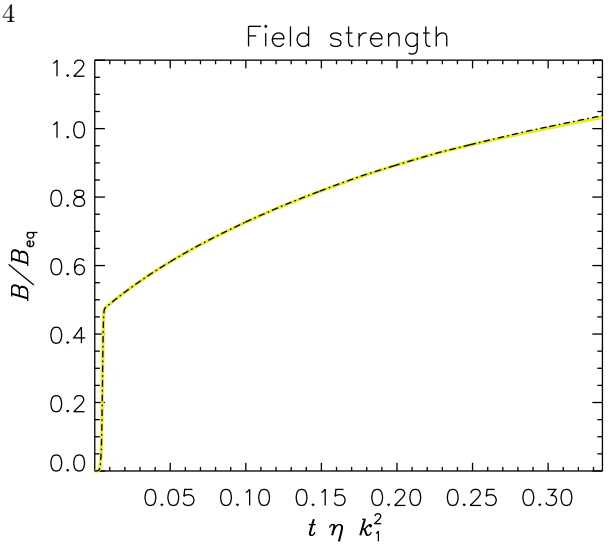

FIG. 1.— Mean-field simulations for an α^2 dynamo at $\mathrm{Re}_M = 10^3$, comparing traditional (yellow/solid/thick) and alternate (black/dashed) dynamical quenching models in a system where they are formally identical.

its existence lies largely on mean-field simulations, which confirm Type 2 quenching for homogeneous isotropic periodic α^2 dynamos. Further, mean-field simulations using traditional α–quenching have strongly suggested the existence of Type 1 quenching for shearing systems.

While we cannot simulate $\alpha^2\Omega$ dynamos at high Re_M, we are in a position to run modest Re_M shearing simulations to compare the predictions of traditional quenching (with and without diffusive magnetic helicity fluxes) with those of alternate quenching. In the latter case, we do not include uncertain diffusive fluxes because the magnetic helicity and therefore α-effect are not expected to exhibit spatial dependencies, which we confirm.

Our procedure then is to run a direct numerical simulation of an $\alpha^2\Omega$ dynamo, extract the spatial dependency of α and compare it with the results of mean-field theories. Once mean-field theories have been weighed against the evidence, we move to large Re_M and examine the evidence for or against Type 1 and 2 quenching.

3. NUMERICS

We perform mean-field numerical simulations for a shearing sheet, with $\boldsymbol{U}_S = Sx\hat{\boldsymbol{y}}$, and averaging performed over the xy plane, so mean quantities are only a function of z, reducing the problem to a one-dimensional one. We use

$$\overline{\boldsymbol{\mathcal{E}}} = \alpha\overline{\boldsymbol{B}} - \eta_t\overline{\boldsymbol{J}}, \tag{17}$$

where η_t is assumed not to be quenched; see Brandenburg et al. (2008a) for a numerical justification of this. The total α is given by the sum of the kinetic α_K, presumed constant, and the magnetic α_M. Accordingly, $\partial\alpha/\partial t = \partial\alpha_M/\partial t$. We solve the two systems of equations

$$\frac{\partial\alpha}{\partial t} = -2\eta_t k_f^2\left(\frac{\overline{\boldsymbol{\mathcal{E}}}\cdot\overline{\boldsymbol{B}}}{B_{\rm eq}^2} + \frac{\alpha-\alpha_K}{\eta_t/\eta}\right) + \mathcal{D}_\alpha\boldsymbol{\nabla}^2\alpha, \tag{18}$$

$$\frac{\partial\overline{\boldsymbol{B}}}{\partial t} = \boldsymbol{\nabla}\times\left(\overline{\boldsymbol{\mathcal{E}}} - \eta\overline{\boldsymbol{J}}\right) \tag{19}$$

for traditional quenching [i.e., Brandenburg & Subramanian 2005, Equations (9.14) and (9.15)] with a diffusive helicity flux with diffusion coefficient $\mathcal{D}_\alpha$, and

$$\frac{\partial\overline{h}}{\partial t} = -2\eta\left(\overline{\boldsymbol{J}}\cdot\overline{\boldsymbol{B}} + \alpha_M B_{\rm eq}^2/\eta_t\right) \tag{20}$$

$$\alpha_M = \eta_t k_f^2(\overline{h} - \overline{\boldsymbol{A}}\cdot\overline{\boldsymbol{B}})/B_{\rm eq}^2 \tag{21}$$

$$\frac{\partial\overline{\boldsymbol{B}}}{\partial t} = \boldsymbol{\nabla}\times\left(\overline{\boldsymbol{\mathcal{E}}} - \eta\overline{\boldsymbol{J}}\right) \tag{22}$$

for alternate quenching. Note that for alternate quenching we also enforce $\int_z \overline{\boldsymbol{A}}\,\mathrm{d}z = 0$ at every timestep to avoid drifts in the magnetic vector potential. The essential difference between the two approaches can be traced back to mutually canceling contributions to the large-scale and small-scale magnetic helicity flux of the form $\mp\overline{\boldsymbol{\mathcal{E}}}\times\overline{\boldsymbol{A}}$.

Our direct numerical simulations are made using the PENCIL CODE, a finite-difference scheme sixth order in space and third order in time. In the PENCIL CODE runs, we use the test-field method (TFM) to determine components of the α tensor as a function of position. For information on TFM, see Brandenburg et al. (2008b) and Brandenburg et al. (2008c).

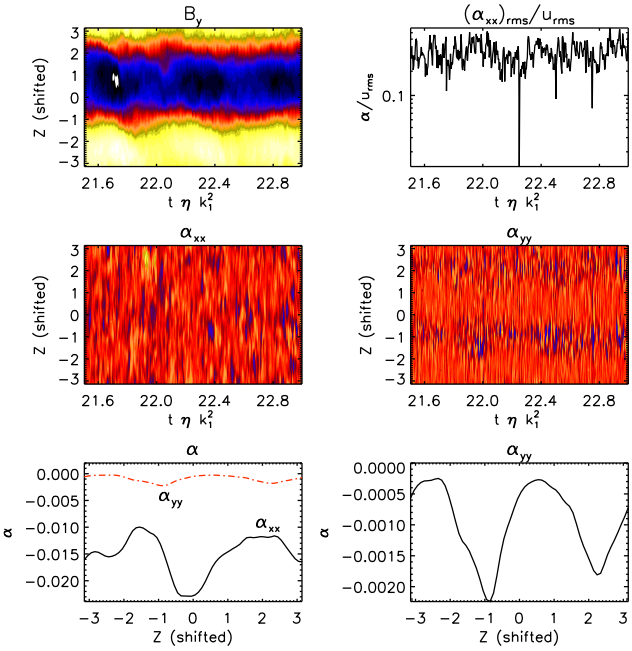

FIG. 2.— α profiles for a direct numerical simulation, well into saturation with $\mathrm{Re}_M = 27$, presented in the frame co-moving with the dynamo wave. Note that the α–quenching is clearly anisotropic, which is beyond the scope of this paper. More importantly, note that the quenching of α_{yy} is nearly uniform.

4. MEASURED α PROFILES

4.1. *Direct simulation*

In Figure 2 we present data for the z dependence of α well into the saturated regime for a direct simulation with $\mathrm{Re}_M = 27$. The butterfly diagrams are shifted to the frame comoving with the traveling dynamo wave, while the bottom panels are time-averages taken in the shifted domains (the quality of which can be estimated from the plot of $\overline{\boldsymbol{B}}_y$). In the top-right panel we show the volume *rms* of α_{xx} in a semi-logarithmic plot. The deep spike marks a reset of the test-fields (Ossendrijver et al. 2002;

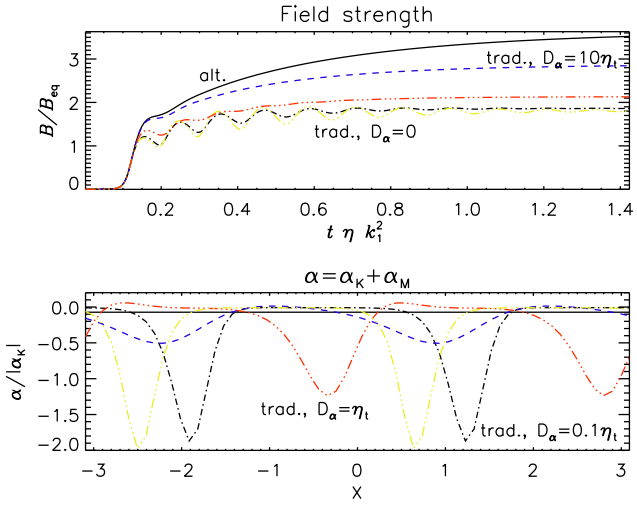

FIG. 3.— Field and $\alpha = \alpha_K + \alpha_M$ (taken at the final time) profiles for mean-field simulations, approximately saturated. Black/solid: alternate quenching formula. Blue/dashed, red, black and yellow/dash–dotted use the conventional quenching formula with $\mathcal{D}_\alpha/\eta_t = 10, 1, 0.1, 0.01, 0$, respectively.

Hubbard et al. 2009). While it may appear from the contour plot that α_{yy} shows spatial variation, when a time average (in the shifted domain) is taken, it is clear that the actual result is that α_{yy} is strongly quenched, and so the spatial variation seen is merely spatial variation in the residual α effect: the quenching is nearly uniform.

We must note here that the quenching is blatantly non-isotropic. A study of this effect is beyond the scope of this paper: we expect it to be a full project in its own right, and intend to study it as such.

4.2. *Mean-field approaches*

In Figure 3 we show energies and α_M profiles for mean-field simulations similar to that of Figure 2 ($\mathrm{Re}_M = 27$, $k_f = 3$). The mean-field simulations are traditional quenching with $\mathcal{D}_\alpha/\eta_t$ ranging from 0 to 10 and a run with alternate quenching. None of the traditional models match the uniform quenching that is measured in Figure 2, showing large spatial variability that derives from the $\overline{\boldsymbol{\mathcal{E}}}\cdot\overline{\boldsymbol{B}}$ term in Equation (14), not even the model with $\mathcal{D}_\alpha = 10\eta_t$. The decrease in spatial variation of α with increasing $\mathcal{D}_\alpha$ suggests that the traditional model could be made to function with an adequate diffusion term, but this term would need to be absurd in scale (and would hopelessly distort any simulation with "real" spatial variation in α_M that needs to be correctly captured). The alternate quenching formalism does result in the uniform quenching, which is unsurprising as it eliminates the spatial forcing from $\overline{\boldsymbol{\mathcal{E}}}\cdot\overline{\boldsymbol{B}}$.

We take this as strong evidence that the alternate quenching formalism is superior to traditional quenching in sheared systems where drifts in $\overline{\boldsymbol{A}}$ are tractable – and that results obtained with traditional quenching in the presence of shear should be viewed with suspicion.

5. MEAN FIELD: LARGE MAGNETIC REYNOLDS NUMBERS

5.1. *Early times*

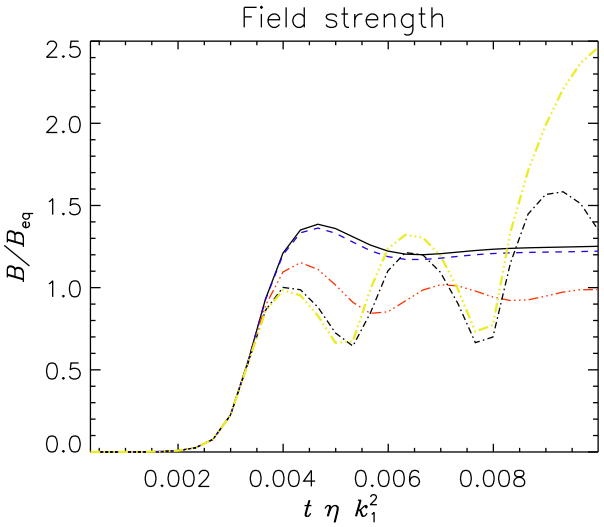

FIG. 4.— Field magnitudes for mean-field simulations, into the non-kinematic regime. Black/solid: alternate quenching formula. Blue/dashed, red, black and yellow/dash–dotted use the conventional quenching formula with $\mathcal{D}_\alpha/\eta_t = 10, 1, 0.1, 0.01, 0$, respectively. Note the oscillations, which persist at some level even with $\mathcal{D}_\alpha = 0.1\eta_t$.

For early times, the predictions of both dynamical α–quenching formalisms predict behavior similar to that of α^2 dynamos: exponential growth of the mean-fields (and corresponding growth of α_M) until the total α effect is reduced enough that the growth rate is reduced to a fraction of its original self. This occurs when $|\alpha| = |2\eta_{\mathrm{T}}^2 k_1^3/S|$, i.e., when

$$\left|\frac{\tau}{3}\langle \boldsymbol{j}\cdot\boldsymbol{b}\rangle\right| = |\alpha_K| - |2\eta_{\mathrm{T}}^2 k_1^3/S|. \tag{23}$$

In terms of magnetic helicity, this becomes

$$|\langle \boldsymbol{a}\cdot\boldsymbol{b}\rangle| = k_f^{-2}\frac{3}{\tau}\left(|\alpha_K| - |2\eta_{\mathrm{T}}^2 k_1^3/S|\right). \tag{24}$$

Using the standard approximations for fully helical turbulence, namely $\tau \simeq 1/u_{\mathrm{rms}}k_f$, $\alpha_K \simeq u_{\mathrm{rms}}/3$ and $\eta_t \simeq \tau u_{\mathrm{rms}}^2/3$, and writing $B_{\mathrm{eq}} = u_{\mathrm{rms}}$, this reduces to

$$|\langle \boldsymbol{a}\cdot\boldsymbol{b}\rangle| \simeq \left(1 - \frac{2k_1^3 B_{\mathrm{eq}}}{3k_f^2|S|}\right)\frac{B_{\mathrm{eq}}^2}{k_f}. \tag{25}$$

As the growth is rapid, we will have $\overline{h}_m \simeq -\overline{h}_f$ during this stage, and so

$$|\overline{h}_m| = \left(1 - \frac{2k_1^3 B_{\mathrm{eq}}}{3k_f^2|S|}\right)\frac{B_{\mathrm{eq}}^2}{k_f}. \tag{26}$$

However, $\alpha\Omega$ dynamo mean-fields are only weakly helical, i.e. $\overline{h}_m \ll \overline{\boldsymbol{B}}^2/k_1$. Under the assumptions that the mean field is approximately stationary, and that the shear is strong enough to use Equation (10) as an approximation, Equation (26) implies that:

$$\langle \overline{\boldsymbol{B}}^2\rangle = \frac{|S|}{2\eta_{\mathrm{T}}k}\overline{h}_m = \left(\left|\frac{S}{2\alpha_K k_1}\right| - \frac{k_1^2}{k_f^2}\right)B_{\mathrm{eq}}^2. \tag{27}$$

As we have made the $\alpha\Omega$ approximation that $|S| \gg |\alpha_K k_1|$, this implies that an $\alpha\Omega$ field first feels nonlinear effects for mean-field energies that are already in super-equipartition.

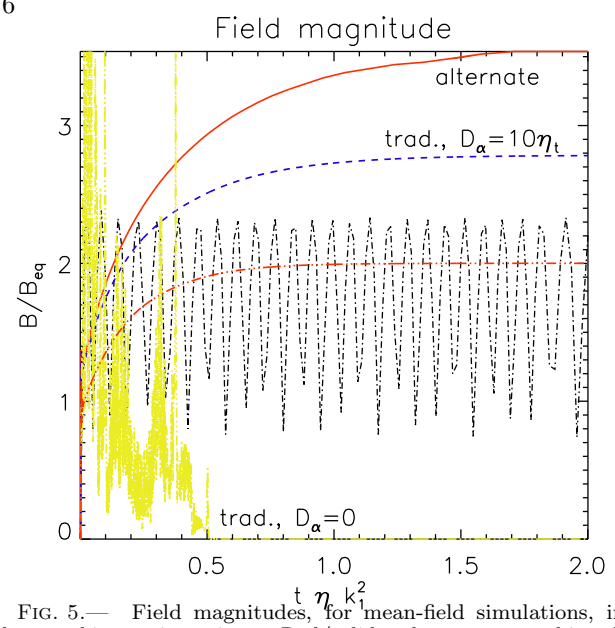

FIG. 5.— Field magnitudes, for mean-field simulations, into the non-kinematic regime. Red/solid: alternate quenching formula. Blue/dashed, red/dash-double-dotted, black/dash-dotted and yellow/dash-double-dotted use the conventional quenching formula with $\mathcal{D}_\alpha/\eta_t = 10, 1, 0.1, 0$, respectively. The curve for $\mathcal{D}_\alpha/\eta_t = 0.1$ is extremely strongly coarse-grained for visibility: the oscillations (for that run) are in fact far more frequent than shown and would be a solid band if plotted fully.

In Figure 4 we show the early evolution of a mean-field dynamo with $\mathrm{Re}_M = 10^3$, $\alpha_K = -1/3$, $S = 1$ and $k_f = 3$. Equation (27) implies that the exit from exponential growth occurs for $\overline{B} \approx 1.18 B_{\rm eq}$, which is well captured by alternate quenching, and traditional quenching with strong diffusive fluxes.

5.2. *Late times*

We can analytically estimate the final field strength of the dynamo for the alternate quenching formalism, while for traditional models the problem is non-linear as can be seen in Figure 3. The final state is achieved when $\partial\overline{h}/\partial t = 0$, i.e., when $\overline{\boldsymbol{J}\cdot\boldsymbol{B}} = \langle \boldsymbol{j}\cdot\boldsymbol{b}\rangle$. Combining this with Equation (10) and assuming that the shear is strong enough that α must be fully quenched $\alpha = \alpha_K + \alpha_M \simeq 0$, we find

$$\overline{\boldsymbol{B}}^2 \simeq |S/2\alpha_K k_1|\,(k_f/k_1)^2 B_{\rm eq}^2. \qquad (28)$$

In Figure 5 we show the late time evolution of the same mean field dynamos. It is clear that without significant ($\mathcal{D}_\alpha > 0.1\eta_t$) helicity diffusion, the solution for traditional quenching is unstable, not surprising as the problem becomes non-linear. However, with moderate diffusion the field strength behaves smoothly, with the final energy level increasing with diffusion coefficient. Even so, the saturation level of the traditional quenching model with $\mathcal{D}_\alpha = 10\eta_t$ is significantly below that of the alternate quenching model. While the diffusion does smooth out the helicity hot-spots, the spatial fluctuations of α_M in Figure 3 have a noteworthy impact on the final dynamo state. Finally, the saturation level of the alternate model matches the estimate from Equation (28) of $\overline{\boldsymbol{B}} \simeq 3.7 B_{\rm eq}$ to within the accuracy limits set by the extremely slow late-time evolution (the change over a time-step is comparable to the rounding errors).

6. DIRECT SIMULATIONS OF OPEN SYSTEMS

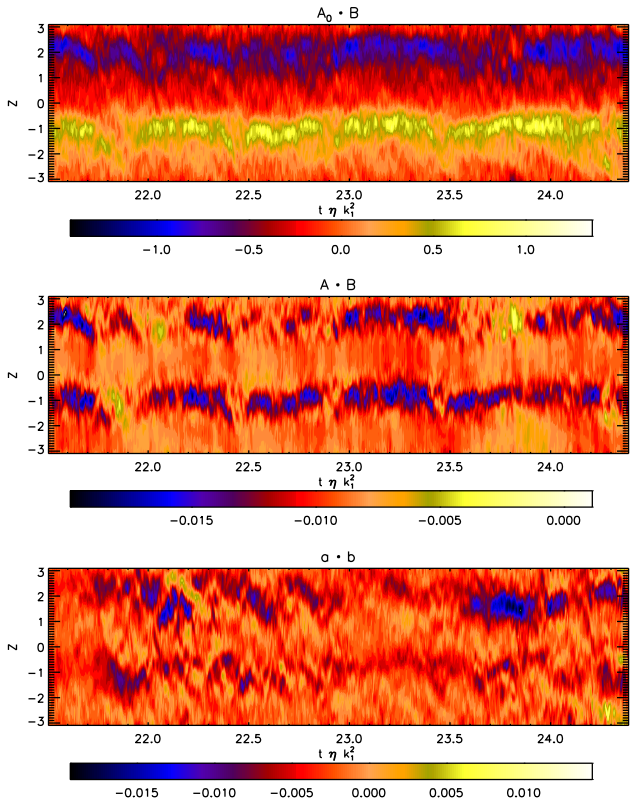

FIG. 6.— Butterfly plots of magnetic helicity. Top panel: $\langle \boldsymbol{A}\rangle_V \cdot \overline{\boldsymbol{B}}$, i.e., the fictitious component of $\overline{h}_m$ due to a spatially homogeneous component of $\boldsymbol{A}$. Middle panel: $\overline{h}_m$, adjusted for the top panel. Bottom panel: $\overline{h}_f$. While there may be some spatial structure in the bottom panels, it is intermittent in time, and the residual from a near-cancellation (the bottom two panels use a very different scale than the top one, see the color bars).

Numerical resources limit our ability to probe the high Re_M regime. However, we have run three simulations of α^2 dynamos in an open system, i.e., a system which can export magnetic helicity. This system is the same one as considered in Brandenburg & Subramanian (2005): a helically forced cube, periodic in the horizontal directions and with vertical field conditions in the vertical directions, which we have run for $\mathrm{Re}_M = 86$ and 156. Additionally, as the vertical field condition is frequently used instead of a proper vacuum condition, we also performed a $\mathrm{Re}_M = 156$ run with potential field condition in the vertical directions. The resulting time series are given in Figure 7. Our resolution was 128^3, for runs with $u_{\rm max} \simeq 0.15$, $u_{\rm rms} \simeq 0.05$ and $\eta = 2\times10^{-4}$ (for $\mathrm{Re}_M = 86$) or $\eta = 10^{-4}$ (for the other two). The velocity boundary has a stress-free vertical condition, and the entropy a symmetric one.

Unlike the results reported in Brandenburg & Subramanian (2005), there is no clear indication of a reduction in the strength of the mean field for higher magnetic Reynolds number, even though the runs were followed for resistive times. However, the use of vertical field conditions as a proxy for vacuum conditions appears to be a poor one. Note that there does not appear to be a slow resistive phase. This lack is expected as the open boundaries allow the system to export total magnetic helicity (not just small-scaled

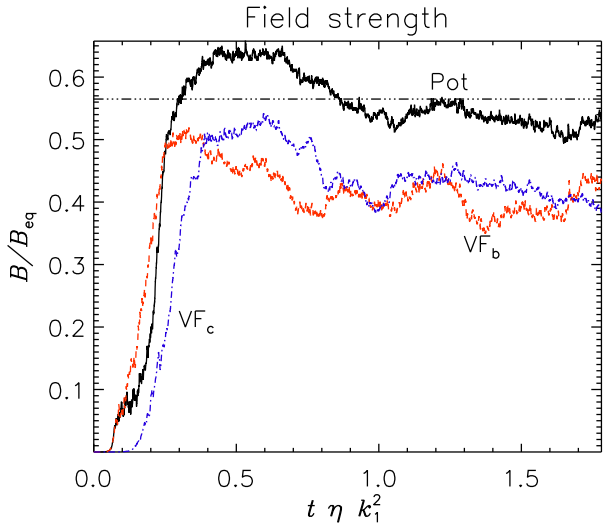

FIG. 7.— Time series for α^2 dynamos in open systems. Black/solid: potential field extrapolation in the vertical direction. Red/blue/dashed: vertical field condition on the vertical direction. Potential field and VF$_b$ have $\mathrm{Re}_M = 156$ while VF$_c$ has $\mathrm{Re}_M = 86$. The dash-double-dotted line corresponds to $1/k_f^{1/2}$, i.e. the energy level associated with the end of the kinematic phase.

helicity). Thus, the system should reach a steady state where exchanges of helicity through the boundary balance preferential destruction of small-scale helicity on dynamical times, and for small total helicities.

7. DISCUSSION AND CONCLUSIONS

We have used the test-field method to examine the predictions of catastrophic α–quenching resulting from dynamically–quenched mean-field models in shearing systems. Formulations for dynamical α–quenching which are superior for the problem of shearing systems do not predict Type 1 catastrophic quenching (reduced field strength) but do predict Type 2 quenching (long final saturation times), extending results that do not allow for spatial variations of α (Blackman & Brandenburg 2002) to models that do. We have further revisited simulations of α^2 dynamos in open systems and, at admittedly quite modest Re_M, found no evidence of field strength scaling inversely with Re_M.

The picture we see now for α–effect dynamos, motivated by the concepts and formalism of dynamical α–quenching, is one of exponential growth during a rapid initial saturation phase. This phase ends when the magnetic helicity in the small-scale fields is comparable to the helicity in the forcing that generates the α–effect. At this point, the total magnetic helicity in the system has not changed from its initial value. If the system is open, exchanges with the exterior (Section 6) will tend to keep the *total* magnetic helicity roughly constant, and the system will then not evolve resistively. On the other hand, if the system is closed the preferential resistive destruction of small-scale magnetic helicity allows a further resistive growth phase.

It is important to note that the energy in the large-scale field is bounded below by its helicity. Weakly helical large-scale fields are possible, which can have super-equipartition fields even at the end of the kinematic growth phase. Weakly helical large-scale fields are a natural product of sheared system, so rapid growth to sub-equi-, equi- and super-equipartition fields are all expected to occur in nature, although all equi- and super-equipartition fields in the high Re_M systems of astrophysics are expected to be weakly helical.

This work was supported in part by the European Research Council under the AstroDyn Research Project 227952. Alexander Hubbard acknowledges the additional support of a fellowship from the Alexander von Humboldt Foundation. The computations have been carried out at the National Supercomputer Centre in Linköping and the Center for Parallel Computers at the Royal Institute of Technology in Sweden.

REFERENCES

Blackman, E. G., & Brandenburg, A. 2002, ApJ, 579, 359
Brandenburg, A. 2001, ApJ, 550, 824
Brandenburg, A., & Dobler, W. 2001, A&A, 369, 329
Brandenburg, A., & Sandin, C. 2004, A&A, 427, 13
Brandenburg, A., & Subramanian, K. 2005, Phys. Rep., 417, 1
Brandenburg, A., & Subramanian, K. 2005, Astron. Nachr., 326, 400
Brandenburg, A., Rädler, K.-H., Rheinhardt, M., & Subramanian, K. 2008a, ApJ, 687, L49
Brandenburg, A., Rädler, K.-H., & Schrinner, M. 2008b, A&A, 482, 739
Brandenburg, A., Rädler, K.-H., Rheinhardt, M., & Käpylä, P. J. 2008c, ApJ, 676, 740
Candelaresi, S., Hubbard, A., Brandenburg, A., & Mitra, D. 2011, Physics of Plasmas, 18, 012903
Cowling, T. G. 1933, MNRAS, 94, 39
Field, G. B., & Blackman, E. G. 2002, ApJ, 572, 685
Guerrero, G., Chatterjee, P., & Brandenburg, A. 2010, MNRAS, 409, 1619
Herzenberg, A. 1958, Royal Society of London Philosophical Transactions Series A, 250, 543
Hubbard, A., & Brandenburg, A. 2010, Geophys. Astrophys. Fluid Dyn., 104, 577
Hubbard, A., & Brandenburg, A. 2011, ApJ, 727, 11
Hubbard, A., Del Sordo, F., Käpylä, P. J., & Brandenburg, A. 2009, MNRAS, 398, 1891
Larmor, J. 1919, Rep. Brit. Assoc. Adv. Sci., 159
Mitra, D., Candelaresi, S., Chatterjee, P., Tavakol, R., & Brandenburg, A. 2010, Astron. Nachr., 331, 130
Ossendrijver, M., Stix, M., Brandenburg, A., & Rüdiger, G. 2002, A&A, 394, 735
Parker, E. N. 1955, ApJ, 122, 293
Pouquet, A., Frisch, U., & Leorat, J. 1976, Journal of Fluid Mechanics, 77, 321
Schrinner, M., Rädler, K.-H., Schmitt, D., Rheinhardt, M., Christensen, U. 2005, Astron. Nachr., 326, 245
Schrinner, M., Rädler, K.-H., Schmitt, D., Rheinhardt, M., Christensen, U. R. 2007, Geophys. Astrophys. Fluid Dyn., 101, 81
Steenbeck, M., Krause, F., Rädler, K.-H. 1966, Zeitschr. Naturforsch. A, 21, 369
Vainshtein, S. I., & Cattaneo, F. 1992, ApJ, 393, 165
Vishniac, E. T., & Cho, J. 2001, ApJ, 550, 752